SC-FDMA Uplink System In Heavily Faded Areas With Low Signal-To-Noise Ratio

Subhra Surochita MISHRA[1], *Jibendu Sekhar ROY*[1]

[1]School of Electronics Engineering, KIIT Deemed to be University, Bhubaneswar, India

subhramishra1991@gmail.com, drjsroy@rediffmail.com

DOI: 10.15598/aeee.v21i3.4987

Article history: Received Dec 22, 2022; Revised Mar 08, 2023; Accepted Aug 24, 2023; Published Sep 30, 2023.

Abstract. *These Single carrier frequency division multiple access (SC-FDMA) has very low power consumption at the sender's side, and it is the access scheme used for the uplink in long-term evolution (LTE). The objective of this work is to explore the error probability of SC-FDMA system under sub-carrier mapping (SM) in heavily faded areas where the signal-to-noise ratios (SNRs) are very low. Wireless environment with heavily faded areas includes military radio systems; direct sequence spread spectrum system (DS-SS), global positioning system (GPS) etc. The localized FDMA (LFDMA) and distributed FDMA (DFDMA) are used to compare the performances of SC-FDMA in heavily faded areas. In heavily faded area with negative signal-to-noise ratio (SNR), the SC-FDMA system is implemented using modulation and encoding methods to receive a very weak signal. Here, binary phase shift keying (BPSK), quadrature phase shift keying (QPSK), 16-PSK, quadrature amplitude modulation (QAM) and 16-QAM modulation techniques are used to calculate the bit error rate (BER) performances. The results show the BER performances of SC-FDMA using mapping schemes for different channels, like, AWGN channel, Rayleigh channel, COST207TU, and COST207RA channel models for heavily faded areas. In AWGN channel, BER at -15dB is about 10 times more than BER at 15dB. The COST207 model shows that the BER is less in typical urban (TU) area compared to the rural area (RA).The performance of BPSK modulation in SC-FDMA system is better in heavily faded areas than other modulation schemes.*

Keywords

Channel models, heavily faded areas, quadrature amplitude modulation, SC-FDMA, sub-carrier mapping.

1. Introduction

Wireless communication has wide applications in fields such as industry, military vigilance, domestic usage, and calamity relief [1]. New advances in communication networks tend to short distance communication through wireless technology. Frequency selective character of the channel of large bandwidth data is the prime barrier for wireless transmission [2], which gives rise to inter-symbol-interference (ISI). To reduce the ISI Orthogonal frequency division multiplexing (OFDM) can be selected for multiple carrier transmission [3]. But it becomes irrelevant in uplink of LTE due to its high PAPR [1]. The vital problems of power consumption in uplink can be resolved by using SC-FDMA where, using discrete Fourier transform (DFT), the symbols are spread over number of subcarriers [4]. Due to the extra blocks, the input signal has low envelope fluctuations in SC-FDMA, hence, it has less PAPR than OFDM which gives more power efficiency [5]. There are different types of mapping techniques i.e., distributed FDMA, localized FDMA and Interleaved FDMA [6]. To deal with the worst-case scenarios the systems need protection when the received signal could be far down to the noise floor. Therefore, to detect signals below the noise floor, signals with negative SNR regimes are used [7]. In the low SNR regime, the number of samples is required to meet specified probabilities of detection and false alarm rate

[8]. It becomes harder for detection below -20 dB but it is possible to detect above it [7].

For SC-FDMA signals, to acknowledge channel fading effect and to obtain BER optimum value, simulations are carried out with Rayleigh faded signal as well as COST207TUx6 and COST207RAx6 models [9]. COST207 (Cooperation in Science and Technology) 207 is a standard of European research union. COST207 model provides scattering characteristics and amplitude statistics in fading environment for typical and bad urban areas, rural areas, and for hilly terrain. The environments which have number of scatters and in direct radio paths, utilize Rayleigh fading channel [9]. The combined space-time block coding and modulation identification in multi-user channel is used in [10] for the SC-FDMA uplink transmission. The power control scheme of lower complexity is reported [11] for non-orthogonal multiple access (NOMA) uplink transmission. Enhanced spectral efficiency of 31.65% is achieved [12] with a multi-user scheduling strategy in non-stand- alone cellular network using MIMO system. A multi-stream cyclic interleaving architecture for interleaved FDMA is used in [13] for the better performance in uplink using simultaneous transmission of multiple data streams.

Literature survey reveals that though SC-FDMA has wide applications in wireless communication but the performance of it, in heavily faded area, is not reported so much. The error probabilities of SC-FDMA under different sub-carrier mapping in heavily faded areas where the SNRs are very low are compared here. Wireless environment with negative SNR includes military radio systems; DS-SS, GPS etc. Also, the BER performances of SC-FDMA System using localized subcarrier mapping scheme with Rayleigh fading distribution as well as COST207TU and COST207RA channel models are evaluated. It is observed that both using LFDMA and DFDMA, BPSK modulation results less BER, specially, in heavily faded areas.

2. SC-FDMA System Model and Channel Models

2.1. SC-FDMA System Model

The block diagram of an SC-FDMA system is presented in Fig. 1 where, cyclic prefix (CP) is used to maintain the orthogonality of subcarriers and works as guard interval (GI). Input symbols are assigned independently to each subcarrier in OFDM but in SC-FDMA each subcarrier is assigned to a signal, combining all data symbols which is modulated and transmitted simultaneously [14]. Before mapping, SC-FDMA has an extra DFT block, with transmitter and receiver

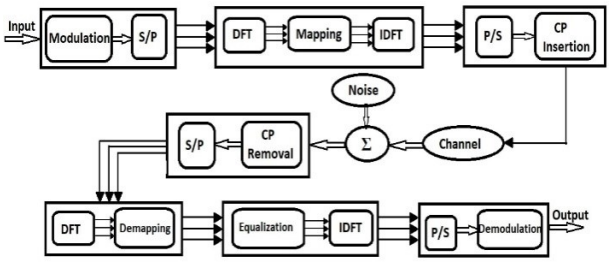

Fig. 1: SC-FDMA system model.

blocks. Here S/P is the serial-to-parallel conversion and P/S is parallel-to-serial conversion. In Table 1, the parameters used are given.

Tab. 1: Parameter Description.

Parameter	Description
U	Total no. of users
P	No. of sub-carriers used
M	Sub-carriers for all user
$D^{(u)}$	Resource allocation matrix
m	Time per sample
$w(m)$	Additive White Gaussian Noise (AWGN)
$h^{(u)}$	Channel Impulse response
L_u	Max. Delay Spread
$h^{(u)}(m,l)$	Sample spaced channel response
L	Total no. of Paths
σ_w^2	Variance
$H(k)$	Frequency-domain channel response
$W(k)$	FT of $w(m)$

First, the information of the source is gathered and mapping is done. For u^{th} user, the input data is transformed to a constellation of symbols and collected into a set of data $s^{(u)}$ having size M. An M-point DFT transforms $s^{(u)}$ to $S^{(u)}$ in frequency domain [15]

$$S^{(u)}(k) = \sum_{m=0}^{M-1} s^{(u)}(m) e^{\frac{-j2\pi mk}{M}}. \quad (1)$$

For $k = 0, 1, \ldots, M-1$, to all the subcarriers, pilots are attached within an exact period, depending on allocation schemes and $S^{(u)}$is mapped to P subcarriers as,

$$X^{(u)} = D^{(u)} \cdot S^{(u)}, \quad (2)$$

for $u = 1, 2, \ldots, U$. After subcarrier mapping, using a P-point IDFT operation, a time-domain signal $x^{(u)}$ is obtained. Then after IDFT, GI is inserted to mitigate the ISI, that is greater than the needed delay spread. By using CP, the signal is modeled and P/S is used. Transmitted signal $x^{(u)}(m)$suffers channel fading [16]. Received signal $y^{(u)}(m)$ is,

$$y^{(u)}(m) = x^{(u)} \otimes h^{(u)}(m) + w(m). \quad (3)$$

After CP removal, the signal transmitted is convoluted circularly to channel IR to give the received sig-

nal. The received signal is,

$$y^{(u)}(m) = \frac{1}{p}\sum_{k=0}^{p-1} x^{(u)}(k) \times \sum_{u=0}^{U-1} H^{(u)}(k,m)e^{\frac{j2\pi mk}{P}} + w(m), \quad (4)$$

where,

$$H(k,m) = \sum_{l=0}^{L-1} e^{\frac{-j\pi lk}{P}}. \quad (5)$$

In frequency domain, after DFT the signal is [17]

$$Y^{(u)}(k) = \sum_{p=0}^{p-1} y^{(u)}(m)e^{\frac{-j2\pi pk}{P}} = x^{(u)}(k)H^{(u)}(k) + W(k), \quad (6)$$

where

$$H(k) = \frac{1}{P}\sum_{k=0}^{P-1} H(k,m), \quad \text{and}$$
$$W(k) = \sum_{p=0}^{P-1} w(m)e^{\frac{-j2\pi pk}{\cdot}P} \quad (7)$$

$\hat{H}^{(u)}(k)$ is the estimated channel and found by removing the pilots. The estimated transmitted signal is,

$$\hat{X}^{(u)}(k) = \frac{Y^{(u)}(k)}{\hat{H}^{(u)}(k)}, \quad (8)$$

For $k = 0, 1, 2, \ldots, P-1$. If frequency domain equalization is done following the de-mapping of sub-carriers, then the de-mapping matrix is

$$R^{(u)} = K^H Y^{(u)} + W. \quad (9)$$

Then M-point IDFT is used for de-mapped symbol and the output signal is,

$$r^{(u)}(m) = \frac{1}{M}\sum_{k=0}^{M-1} R^{(u)}(k)e^{\frac{j2\pi mk}{M}}. \quad (10)$$

In the demodulation block IDFT output is used and the final bit stream is generated by the receiver. The resulting signal is sent to IDFT but a complex equalizer is used before that [18].

2.2. Channel Models

In this work, three types of channel models are used, which are AWGN channel, Rayleigh channel and COST207 channel (typical urban and rural areas). The Rayleigh channel follows a zero-mean Gaussian distribution [19]. Rayleigh distribution is the statistical nature or probability distribution function (PDF) for multipath fading in wireless communication. COST207 model provides scattering and amplitude characteristics in fading environment for urban areas, rural areas including hilly terrain. The BER performance of SC-FDMA system with these channel models are investigated. Suppose X_1 and X_2 are Gaussian random variables having zero mean. Let σ^2 is the variance and R_{Ray} is the amplitude of the random variable and is given by,

$$R_{Ray} = \sqrt{X_1^2 + X_2^2}, \quad (11)$$

Where, R_{Ray} follows a Rayleigh distribution whose density is, $f_(R_{Ray})(x) = x/\sigma^2 e^{\frac{x^2}{2\sigma^2}}$. For $x \in \mathrm{R}$ and $x \geqslant 0$, σ depends on the width of the density function.

In mobile networks, fading is often modeled using Rayleigh random variables [20]. Channel models describe the characteristics of the link connecting the transmitter and receiver which bears data in the form of electromagnetic waves [21]. In this work, the multipath fading is only considered owing to the useful and harmful combination of different types of signal components. This is fast fading case and is the cause of short-term fading [22]. Next different scenarios are analyzed where the fast fading follows frequency selective Rayleigh, AWGN channel and COST207 model for rural and urban areas.

For modeling a frequency selective fading channel, the power delay profile (PDP) of the fading channel model provides average power distribution for received signal over the individual path [23]. So far, COST207 has been widely recognized as one of the most popular and practical PDP models [24]. The power delay profile for COST207 is for typical Rural area,

$$PDP = \begin{cases} 9.21e^{-9.2\tau}, & 0 \leqslant \tau < 0.7 \\ 0, & \text{else} \end{cases}. \quad (12)$$

For typical Urban area,

$$PDP = \begin{cases} e^{-\tau}, & 0 \leqslant \tau < 7 \\ 0, & \text{else} \end{cases}. \quad (13)$$

3. Performance of SC-FDMA in Heavily Faded Areas

This part verifies the performance of the SC-FDMA system model through simulation and comparison of the mapping schemes and channel models. Here, the simulation parameters are generated using MATLAB

and given in Table 2. The simulation is run for N-total subcarriers i.e., 128, 256, 512 and 1024, for each user number of accessible subcarriers is 64, spreading factor Q is 4, and cyclic prefix length $P = 16$. The number of users are 2,4 and 8 and the sampling period of the channel is 1e-3. Number of SC-FDMA frames is 10^3. The Simulink model is simulated in MATLAB over different fading channels for uplink with different size of FFT, modulation techniques and mapping schemes. The baseband channel models are used to model the system. When the FFT size is 128, the simulation time is about 2 minutes whereas the simulation time for FFT size of 1024 it is about 15 minutes. To implement the SC-FDMA system model of Fig. 1, in programming, first the signal is modulated and converted from serial to parallel. Then after DFT, the sub-carrier mapping is implemented and before CP insertion, parallel to serial conversion is done. Then the signal is passed through the channel under noise and CP is removed. Then after serial to parallel conversion, the demapping is done. After equalization, the signal is passed through the IDFT block and then it is demodulated to obtain the output.

Tab. 2: Simulation Specifications.

Parameters	Specifications
FFT Size	128, 256, 512 and 1024
Modulation	Type QAM, BPSK, QPSK, 16-QAM, 16-PSK
Cyclic Prefix	16
No. of Symbols	100
SNR	-15 to 15
Mapping Technique	Localized, Distributed
Channel Model	Rayleigh, AWGN, COST207TU, COST207RA
Path Delay	$[01e-53.5e-512e-5]$dB
Path Gain	$[0-1-1-3]$ns

In Fig. 2, two different cases of mapping distributions of SC-FDMA, in a frequency selective AWGN channel with varying the SNR values i.e., both positive and negative SNR is shown, where it can be seen that the BER is nearly 10−1 for both localized and distributed schemes.

By varying the user number (U), the performance of LFDMA and DFDMA is compared and shown in Fig. 3.

In Fig. 4, two different cases where the fast fading follows different distributions, in a frequency selective AWGN channel with varying the SNR values i.e., both positive and negative SNR is shown for BPSK and QAM modulation using LFDMA.

Then the error probability is evaluated for a Rayleigh fading channel, which is frequency-selective and represented by the impulse response coefficients of the channel i.e., $i = (i(1), i(2) \ldots i(n))$, where all coefficients are assumed to be circularly symmetric complex Gaussian

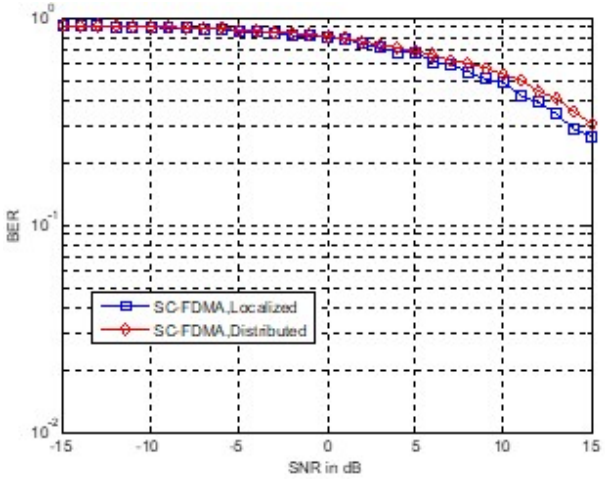

Fig. 2: BER performance for localized and distributed mappings for AWGN channel.

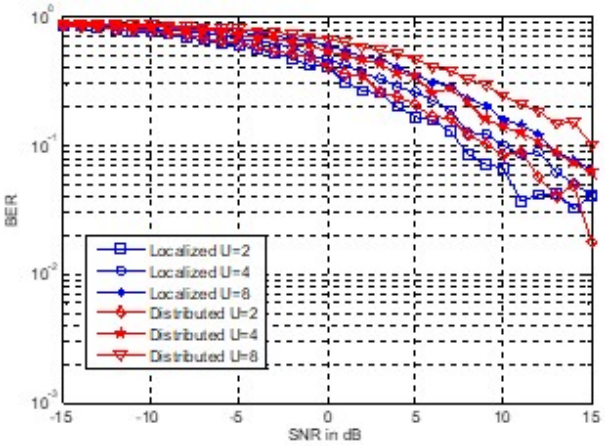

Fig. 3: BER performance for AWGN channel.

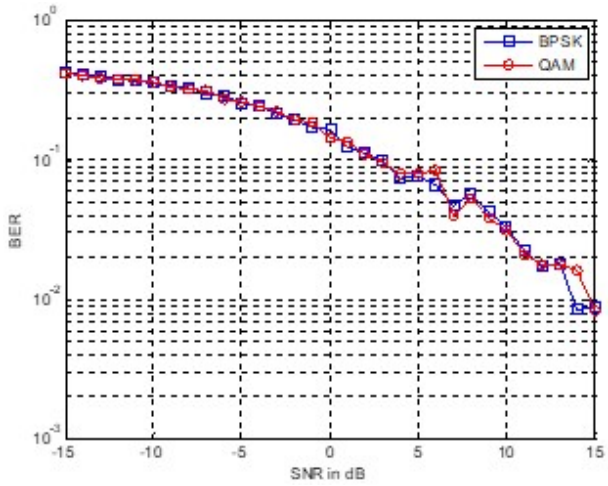

Fig. 4: BER vs SNR plot for BPSK and QAM for AWGN channel.

Tab. 3: Comparison of Result.

Paper	Parameters	Channel/Equalizer	Mapping	Signal-to-noise ratio	Bit Error Rate
Ref [23] S. Ebadinezhad	N=256 SM=Localized, Interleaved SNR=0 to 20 CP=20	AWGN, ZFE	Localized	0dB	$10^{-0.5}$
				14dB	10^{-6}
			Interleaved	0dB	$10^{-0.5}$
				14dB	10^{-6}
		AWGN, MMSE	Localized	0dB	$10^{-0.5}$
				14dB	10^{-6}
			Interleaved	0dB	$10^{-0.5}$
				14dB	$10^{-5.5}$
		Rayleigh, ZFE	Localized	0dB	$10^{-0.5}$
				15dB	10^{-3}
			Interleaved	0dB	$10^{-0.5}$
				15dB	$10^{-3.5}$
		Rayleigh, MMSE	Localized	0dB	$10^{-0.4}$
				15dB	10^{-2}
			Interleaved	0dB	$10^{-0.4}$
				15dB	10^{-2}
Ref [14] R. Chisab	N=128 to 2048 SM=Localized, Distributed SNR=0 to 20 7 for normal CP and 6 for extended CP	ZF	Localized	0dB	10^{-1}
				8dB	10^{-4}
		MMSE	Localized	0dB	10^{-1}
				7dB	10^{-4}
		COST207	Localized (RA)	8.2dB	10^{-3}
			Localized (TU)	7.5dB	10^{-3}
			Distributed (RA)	11dB	10^{-3}
			Distributed (TU)	11.5dB	10^{-3}
Ref [25] M. Al. Rawi	SC-FDMA, OFDMA SM=Localized, Interleaved SNR=0 to 30	ITU vehicular-A MMSE	OFDMA Localized (QPSK)	0dB	10^{0}
				15dB	10^{-1}
			OFDMA Localized (16 QAM)	0dB	10^{0}
				15dB	10^{-2}
			OFDMA Interleaved (QPSK)	0dB	10^{0}
				15dB	10^{-1}
			OFDMA Interleaved (16 QAM)	0dB	10^{0}
				15dB	10^{-2}
			SC-DMA Localized (QPSK)	0dB	10^{0}
				15dB	10^{-2}
			SC-DMA Localized (16 QAM)	0dB	10^{0}
				15dB	10^{-1}
			SC-FDMA Interleaved (QPSK)	0dB	10^{0}
				15dB	10^{-1}
			SC-FDMA Interleaved (16 QAM)	0dB	10^{0}
				15dB	10^{-3}

random variables with $CN(0,1)$ distribution. In Fig. 5, the BER is estimated for each SC-FDMA transmitted symbol in a Rayleigh fading channel. After the IDFT process, the resulting output is an upsampled version of the original sequence In Fig. 5 the comparison of BPSK and QAM modulation scheme is simulated by varying the SNR from -15 dB to 15 dB. Heavily faded area is considered where SNR is negative.

The BER performance of Rayleigh channel of Fig. 5 is not as good as the performance like the AWGN channel (Fig. 4), because the Rayleigh channel considers multipath fading.

In Fig. 6, the BER performance comparison between TU model and RA model with channel object = 6 is shown.

At 15dB, the COST207TU model obtained a BER of $10^{-2.1}$ but a BER of less than $10^{-2.1}$ is observed for the COST207RA model with positive SNR and the COST207TU model obtained a BER of $10^{-2.02}$ but a

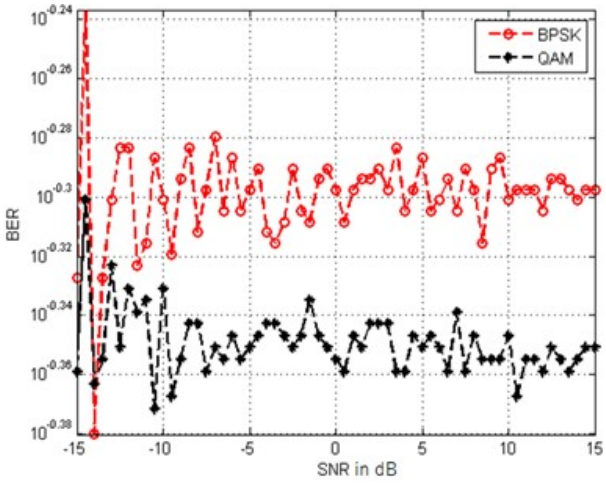

Fig. 5: BER performance for BPSK and QAM for Rayleigh channel.

Tab. 4: Our Result.

This Paper	N=128, 1024 SM=Localized, Distributed SNR=-15 to 15, CP=16	AWGN	Localized (U=2)	-15dB	10^{0}
				0dB	$10^{-0.5}$
				15dB	10^{-2}
			Localized (U=4)	-15dB	10^{0}
				0dB	$10^{-0.5}$
				15dB	$10^{-1.5}$
			Localized (U=8)	-15dB	10^{0}
				0dB	$10^{-0.5}$
				15dB	10^{-1}
			Localized (BPSK)	-15dB	10^{0}
				0dB	10^{-1}
				15dB	10^{-2}
			Localized (QAM)	-15dB	10^{0}
				0dB	10^{-1}
				15dB	10^{-2}
			Distributed (U=2)	-15dB	10^{0}
				0dB	$10^{-0.5}$
				15dB	10^{-2}
			Distributed (U=4)	-15dB	10^{0}
				0dB	$10^{-0.5}$
				15dB	10^{-1}
			Distributed (U=8)	-15dB	10^{0}
				0dB	10^{0}
				15dB	10^{-1}
		Rayleigh	Localized (BPSK)	-15dB	$10^{-0.32}$
				0dB	$10^{-0.3}$
				15dB	$10^{-0.3}$
			Localized(QAM)	-15dB	$10^{-0.36}$
				0dB	$10^{-0.36}$
				15dB	$10^{-0.34}$
		COST207	Localized (RA)	-15dB	$10^{-2.04}$
				0dB	$10^{-2.04}$
				15dB	$10^{-2.1}$
			Localized (TU)	-15dB	$10^{-2.02}$
				0dB	$10^{-2.04}$
				15dB	$10^{-2.1}$

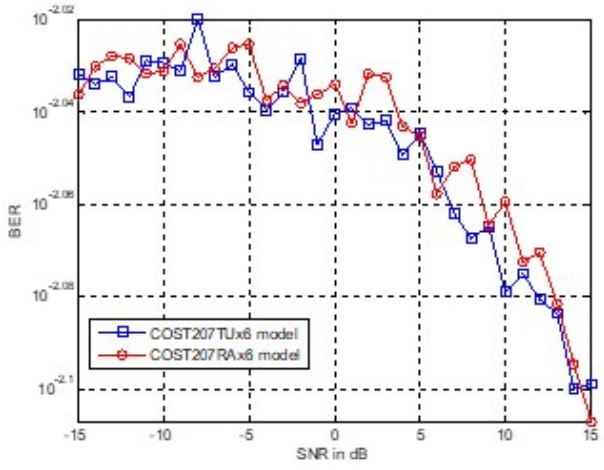

Fig. 6: BER performance for rural area and typical urban in COST207x6 channel.

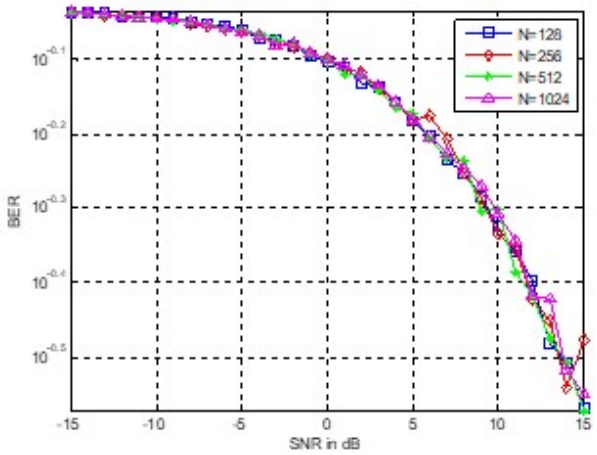

Fig. 7: Performance of BER for different number of sub-carriers using LFDMA.

$10^{-2.04}$ BER is observed for the COST207RA model with negative SNR at -15dB. The BER is less in case of a RA model than the TU model.

The Variation of BER with different number of sub-carriers (N) for 16-PSK modulation in LFDMA is shown in Fig. 7.

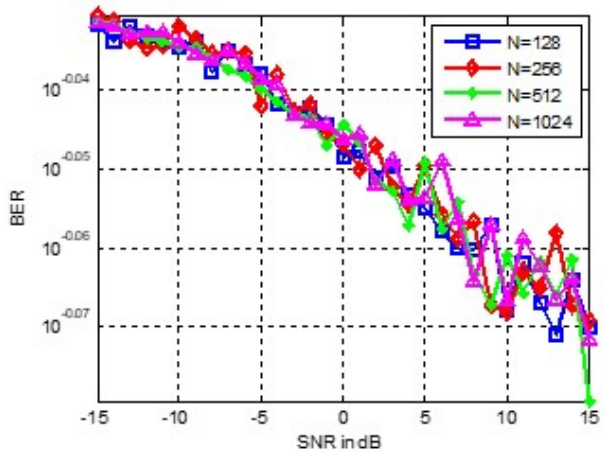

Fig. 8: Performance of BER for different number of sub-carriers using DFDMA.

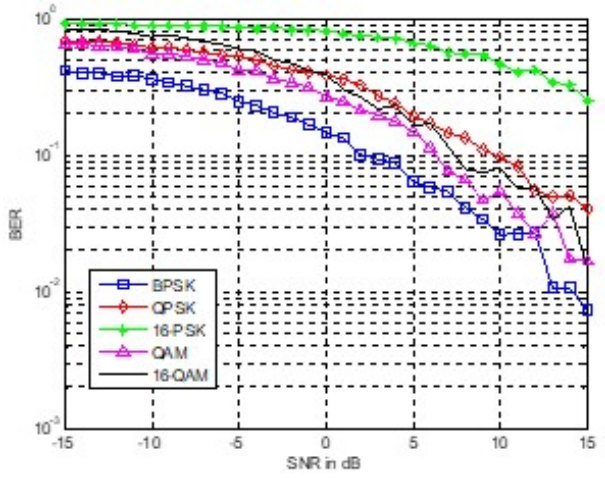

Fig. 9: Performance of BER for different types of modulation for LFDMA.

From the above figure it is observed that in heavily faded areas (negative SNR region) the BER performance does not depend so much on the sub-carrier number. The variation of BER with different sub-carrier number for 16-PSK modulation using DFDMA is plotted in Fig. 8.

From the above figure it is observed that in heavily faded areas (negative SNR region) with DFDMA the BER performance does not depend so much on the sub-carrier number. The variation of BER with different modulation schemes in LFDMA is presented in Fig. 9.

From the Fig. 9, it is observed that LFDMA with BPSK results low BER of about 10-2 compared to all other modulation schemes, and a high BER is observed in case of 16-PSK. So, from the figure it is observed that in heavily faded areas (negative SNR region) the BER performance is better for BPSK modulation.

Variation of BER with different modulation schemes for DFDMA is shown in Fig. 10.

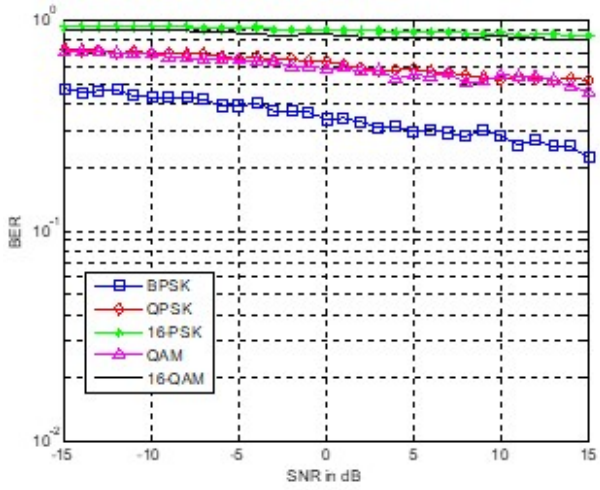

Fig. 10: Performance of BER for different types of modulation for DFDMA.

From the Fig. 10, it is found that DFDMA with BPSK results low BER of about 10^{-1} compared to all other modulation schemes, and a high BER are observed in case of 16-PSK and 16-QAM. So, from the Fig. 9 and Fig. 10 it is observed that in heavily faded areas (negative SNR region) the BER performance is better for BPSK modulation. Both in Fig. 9 and Fig. 10, AWGN channel is used.

The simulated results are compared with the published results [14], [23], [25] in Table 3 and Table 4. In these reports zero forcing equalizer (ZFE) and maximum mean square error (MMSE) equalizer are used. The channels used are AWGN, Rayleigh, COST207 and ITU-vehicular-A

By comparing both the mapping schemes it is obtained that LFDMA has better BER than DFDMA. Also, it is compared by varying the number of users. By taking different number of sub-carriers and varying the modulation technique the BER performance is shown for both the mapping schemes. In Table 3, the simulated results are compared with the published results for positive SNR (due to the unavailability of results in the heavily faded areas with negative SNRs). The results, presented in this paper, show that in the heavily faded areas the BER performance detoriates drastically for all types of sub-carrier mappings and for all the channels, like, AWGN, Rayleigh and COST207.

4. Conclusion

The BER performance of the SC-FDMA System in heavily faded area is presented. The localized and distributed sub-carrier mapping scheme are used with AWGN channel, Rayleigh fading channel as well as COST207TU and COST207RA channel models. The

BER obtained using LFDMA with BPSK and QAM modulations for AWGN channel is 10^{-2} for SNR of 15dB. Then the system is run for Rayleigh fading channel as well as COST207TU and COST207RA channel models. With channel object = 6 at 15 dB, for COST207TU model BER of $10^{-2.1}$ is obtained. But a BER of less than $10^{-2.1}$ is observed for the COST207RA model with positive SNR. Using COST207TU and COST207RA models BER of $10^{-2.02}$ and $10^{-2.04}$ are obtained respectively for negative SNR of -15dB. The comparison between the COST207TU and COST207RA models shows that the BER is less in the TU model compared to the RA model. Because of the unavailability of research reports on SC-FDMA system in heavily faded area with negative SNR, the results could not be compared with published papers. The BER performance in heavily faded area, considering the energy efficiency of SC-FDMA system will be the future work. Another future work is to continue this work by using discrete cosine transform SC-FDMA (DCT-SC-FDMA) model for the investigation of performance in the heavily faded areas.

Author Contributions

S. S. M. has contributed to develop the theory, program code and simulated the system to provide the results. J. S. R. has supervised the whole work, edited the paper, and edited the plagiarism matter. Both S. S. M. and J. S. R. have contributed for the final version of the paper.

References

[1] CHO, Y. S., J. KIM, W.Y. YANG and C.G. KANG. *MIMO-OFDM Wireless Communications with MATLAB*. John Wiley & Sons (Asia) Pte Ltd, 2010. ISBN 978-0-470-82561-7..

[2] MYUNG, H. G. Introduction to single carrier FDMA. *In: 15th European Signal Processing Conference (EUSIPCO)*. 2007, pp. 2144-2148. ISBN 978-83-921340-2-2. Available at: https://ieeexplore.ieee.org/document/7099187.

[3] JAWHAR, Y. A., et.al. Improving PAPR performance of filtered OFDM for 5G communications using PTS. *ETRI Journal Wiley*. 2021, vol. 43, iss. 2, pp. 209-220.ISSN 2233-7326. DOI: DOI: 10.4218/etrij.2019-0358.

[4] KAMATHAM,Y. and S. POLLAMONI. Implementation of OFDM System with Companding for PAPR Reduction using NI-USRP and LabVIEW. *In:2019 IEEE International WIE Conference on Electrical and Computer Engineering (WIECON-ECE)*. 2019, pp. 1-4.ISBN 978-1-7281-4499-3 DOI: 10.1109/WIECON-ECE48653.2019.9019946.

[5] KHAN, M., S. IQBAL and W. ASGHAR. A Review paper on: The PAPR analysis of OFDM systems. *International journal of Mobile Network Communications & Telematics (IJMNCT)*. 2014, vol. 04, iss. 1, pp. 1-13.ISSN 1839-5678. DOI: 10.5121/ijmnct.2014.4101.

[6] NAIDU, G. R.and V. M. RAO. Performance evaluation of companded localized FDMA for LTE uplink communications. *SN Applied Sciences, A Springer Nature Journal*.2020, vol. 2, iss. 7, pp. 1291.ISSN 2523-3971. DOI: 10.1007/s42452-020-3092-6.

[7] CABRIC, D. Addressing the Feasibilityof Cognitive Radios. *IEEE Signal Processing Magazine*. 2008, vol. 25, iss. 6, pp. 85-93.ISSN 1053-5888. DOI: 10.1109/MSP.2008.929367.

[8] CHUNG, K. H.On Negative Correlation Bit-to-Symbol(B2S) Mapping for NOMA with Correlated Information Sources in 5G Systems. *Journal of the KIECS*. 2020, vol. 15, iss, 5, pp. 881-888. ISSN 1975-8170. DOI: 10.13067/JKIECS.2020.15.5.881.

[9] [9] MYUNG, H. G., J. LIM and D. J. GOODMAN. Single carrier FDMA for uplink wireless transmission. *IEEE Vehicular Technology Magazine*. 2006,vol. 11, iss. 1, pp. 30-38.ISSN 1556-6072. DOI: 10.1109/MVT.2006.307304.

[10] MAREY, M. and H. MOSTAFA. A Powerful Joint Modulation and STBC Identification Algorithm for Multiuser Uplink SC-FDMA Transmissions. *Applied Sciences*, 2023, vol. 13, iss. 3, 1853, pp. 1-18. ISSN 2076-3417. DOI: 10.3390/app13031853.

[11] REHMAN, B. U. et. al. Uplink Power Control Scheme for Spectral Efficiency Maximization in NOMA systems. *Alexandria Engineering Journal*, 2023, vol. 64, pp. 667-677. ISSN 1110-0168. DOI: 10.1016/j.aej.2022.11.030.

[12] KUKADE, S., M. S. SUTAONE and R. K. PATIL. Uplink Transmission With Multiuser Scheduling in Non-Stand-alone Cellular Network using Virtual MIMO System. *Transactions on Emerging Telecommunications Technologies*, 2023, vol. 34, iss. 1, e4649. ISSN 2161-3915. DOI: 10.1002/ett.4649.

[13] KUMAR, J. A. and S. L. STUWART. Intersymbol Interference Resilient Interleaving Architec-

ture for Multi-Stream Interleaved Frequency Division Multiple Access System. *International Journal of Communication Systems*, 2023, vol. 36, iss. 3, e5394. ISSN 1099-1131 DOI: 10.1002/dac.5394.

[14] CHISAB, R. F. and C. K. SHUKLA. Comparative study in performance for subcarrier mapping in uplink 4G-LTE under different channel cases. *International Journal of Advanced Computer Science and Applications*. 2014, vol. 05, pp. 46-54.ISSN 2156-5570. DOI: 10.14569/IJACSA.2014.050107.

[15] MAHIND, U. and M. KADAM. BER Performance of OFDM System in Noise and Fading Channel for Modified SL0 Sparse Algorithm. *Journal of Telecommunications System & Management*. 2016,vol. 5, iss. 3, pp-363-368.ISSN 2167-0919. DOI: 10.1109/ICGTSPICC.2016.7955329.

[16] BANDOPADHAYA,S. and J. S. ROY. *Spectral efficiency in wireless networks through MIMO-OFDM system*, Chapter-10, Handbook of Research on Advanced Wireless Sensor Network Applications, Protocols and Architectures, IGI Global, 2017, pp. 249-277.ISSN 2327-3313.

[17] FALCONER,D., S. L. ARIYAVISITAKUL, A. B. SEEYAR and B. EIDSON. Frequency domain equalization for single-carrier broadband wireless systems. *IEEE Communications Magazine*. 2002,vol. 40, pp. 58-66.ISSN 0163-6804 DOI: 10.1109/35.995852.

[18] CIMINI, L. J. J. Peak-to-average power ratio reduction of an OFDM signal using partial transmit sequences. *IEEE Communications Letters*. 2000, vol. 4, iss. 3,pp. 86-88.ISSN 1089-7798. DOI: 10.1109/4234.831033.

[19] NOUNE, M. and A. NIX. Frequency-Domain Precoding for Single Carrier Frequency-Division Multiple Access. *IEEE Communications Magazine*. 2009, vol. 47, iss. 6,pp. 68-74.ISSN 0163-6804. DOI: 10.1109/MCOM.2009.5116802.

[20] [20] RAMTEJ,S. and S. ANURADHA. On Companding Techniques to mitigate PAPR in SC-FDMA systems. *International Journal of Wireless and Mobile Computing*. 2020,vol. 18, iss. 3, pp. 295-302.ISSN 1741-1092. DOI: 10.1504/IJWMC.2020.10028074.

[21] CHAFII, M., F. BADER and J. PALICOT. SC-FDMA with Index Modulation for M2M and IoT Uplink Applications. *IEEE Wireless Communications and Networking Conference (WCNC)*. 2018, pp. 1-5.ISBN 978-1-5386-1734-2. DOI: 10.1109/WCNC.2018.8377028.

[22] KASEM, E. and R. MARŠALEK. The Performance of LTE Advanced Uplink in Flat Rayleigh and Pedestrian Channels. *Elektro Revue*. 2013, vol.4, iss. 3, pp.45-50.ISSN 1213-1539. DOI: 10.3906/elk-1908-163.

[23] [EBADINEZHAD, S. and S. HASAN. BER Evaluation in LTE SC-FDMA under Multipath Channels. *International Journal of Recent Technology and Engineering (IJRTE)*. 2019, vol.8, iss. 4, pp. 3539-3547.ISSN 2277-3878. DOI: 10.35940/ijrte.D7767.118419.

[24] MUSA, A. M., R. A. MOKHTAR, R. A. SAEED, H. ALHUMYANI, S. ABDEL-KHALEK and A. O. U. MOHAMED. Distributed SC-FDMA sub-carrier assignment for digital mobile satellite. *Alexandria Engineering Journal, Elsevier*. 2021,vol. 60, iss. 6, pp. 4973-4980. ISSN 1110-0168. DOI: 10.1016/j.aej.2021.04.064.

[25] RAWI, M. Al. Performance Analysis of OFDMA and SC-FDMA. Int. Rev. Appl. *Sci. Eng.* 2017, vol. 08, iss. 02, pp. 113–116.ISSN 2062-0810. DOI: 10.1556/1848.2017.8.2.2.

About Authors

Subhra Surochita MISHRA was born in Balangir, Odisha, India. She is a full-time Research Scholar in the School of Electronics Engineering, KIIT University, Bhubaneswar, India. She has received her B. Tech degree from MITS, Rayagada, India and M. Tech degree from Silicon Institute of Technology, Bhubaneswar, India. Her areas of research work are SC-FDMA, MIMO and she is pursuing her Ph. D.

Jibendu Sekhar ROY (corresponding author) is a full professor and Ex-Associate Dean, School of Electronics Engineering, KIIT University, Bhubaneswar, Odisha. Earlier he was a professor in the ECE department, BIT, Mesra, Ranchi from 1998-2009. He has received MSc in Physics (Radio Ph & Electronics) from The University of Burdwan, WB. He has received his Ph. D. degree from Jadavpur University, Calcutta and was a CSIR (Gov. of India) Research Associate. He was a Post-Doctoral Research Associate of CNRS (Gov. of France), France. He has published about 250 papers in international journals and symposia, guided 45 M. Tech. Theses and 10 Ph. D. Theses. He has visited France, USA, Italy, Indonesia, Denmark, Czech Republic, South Korea, Russia and Bali for paper presentation/invited talk/session chair. He was one of the members of the EAGER-NETWIC Project of ASIA LINK Program during 2001-2004. He is a life member of ISTE (India), and ISCA (India), IAENG (USA), JSPS (Japan). Dr. Roy was awarded by the

Senior Associateship of ICTP (UNESCO), Trieste, Italy in 2008. The name of Dr JS Roy has been listed in Marquis World Who's Who.